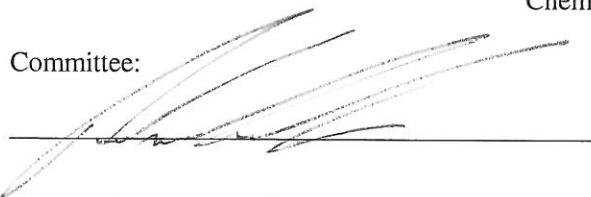


Francisella tularensis IspD: A Target for Novel Antibiotics

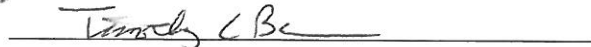
by

Arthur Tsang  
A Thesis  
Submitted to the  
Graduate Faculty  
of  
George Mason University  
in Partial Fulfillment of  
The Requirements for the Degree  
of  
Master of Science  
Chemistry

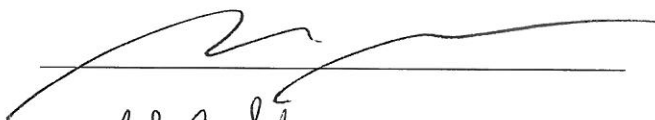
Committee:



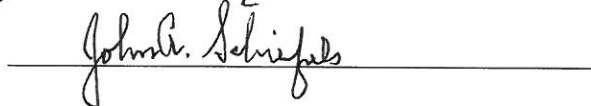
Dr. Robin Couch, Thesis Director



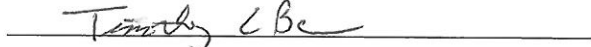
Dr. Timothy L. Born, Committee Member



Dr. Barney Bishop, Committee Member



Dr. John Schreifels, Department Chairperson



Dr. Timothy L. Born, Associate Dean for Student and Academic Affairs, College of Science



Dr. Vikas Chandhoke, Dean, College of Science

Date: December 7, 2012

Fall Semester 2012  
George Mason University  
Fairfax, VA

*Francisella tularensis* IspD: A Target for Novel Antibiotics

A thesis submitted in partial fulfillment of the requirements for the degree of Master of Science at George Mason University

By

Arthur Tsang  
Bachelor of Science  
George Mason University, 2009

Director: Robin Couch, Professor  
Department of Chemistry and Biochemistry

Fall Semester 2012  
George Mason University  
Fairfax, VA

Copyright: 2012 Arthur Tsang  
All Rights Reserved

## **Dedication**

This is dedicated to all who have contributed to my education.

## **Acknowledgements**

Dr. Robin Couch, for mentoring me during this research.

Dr. Timothy Born and Dr. Barney Bishop for taking the time to critique my work and serve on my committee.

Dr. Weidong Zhou at the Center for Applied Proteomics and Molecular Medicine, George Mason University, Manassas, VA performed the phosphopeptide analysis work.

Ms. Amy Fisher, Center for Nanophotonics Imaging, George Mason University, for guiding me through fluorescence spectroscopy.

Mr. Thomas Huff and Ms. June Liu of the Shared Research Instrument Facility (SRIF) at George Mason University guided me through mass spectrometry analysis during the bioprospecting experiment.

Ms. Jessica Crable, Mr. Brian Colchao, for their work on this project.

## Table of Contents

	Page
List of Tables .....	vi
List of Figures .....	vii
Abstract .....	viii
Introduction .....	1
Experimental Aims .....	12
Materials and Methods .....	15
Results and Discussion .....	23
Conclusion .....	41
References .....	43
Curriculum Vitae .....	49

## List of Tables

Table	Page
1: Kinetic results of IspD assays .....	27
2: Active site residues of <i>E. coli</i> IspD conserved in <i>F. tularensis</i> IspD .....	33

## List of Figures

Figure	Page
1: Schematic of the mevalonate pathway.....	5
2: Schematic of the methylerythritol phosphate pathway.....	6
3: Fosmidomycin and FR900098.....	8
4: Schematic of IspD Assay.....	18
5: Vector map of <i>F. tularensis</i> IspD in pET101d.....	24
6: Vector map of <i>E. coli</i> IspD cloned into pET28c.....	24
7: SDS-PAGE result of IspD purification.....	25
8: Initial velocity measurements of <i>F. tularensis</i> IspD.....	26
9: Initial velocity measurements of <i>E. coli</i> IspD for MEP.....	26
10: Microtitre plate assay showing visibility of colorimetric assay.....	28
11: IspD metal ion preference.....	29
12: IspD nucleotide preference in 200 $\mu$ M MEP.....	31
13: IspD nucleotide preference in 400 $\mu$ M MEP.....	31
14: Active site residues of <i>E. coli</i> IspD.....	35
15: <i>F. tularensis</i> IspD predicted dimer.....	36
16: Molecular masses of IspD, T141D, T141E by size exclusion.....	37
17: Relative activity of the IspD T141D and T141E mutants.....	38
18: Intrinsic fluorescence of wild type, T141D, and T141E IspD.....	38
19: Activity of IspD before and after bioprospecting.....	40



## Abstract

*Francisella tularensis* IspD: A Target for Novel Antibiotics

Arthur Tsang, MS

George Mason University, 2012

Thesis Director: Dr. Robin Couch

*Francisella tularensis* is the pathogenic bacteria responsible for causing Tularemia, a severe disease that has been explored as a biological weapon, leading to its classification as a Category A bioterrorist agent. To facilitate the development of novel therapeutics against *F. tularensis*, we investigated the metabolic enzyme IspD, which catalyzes an early intermediate step in the 2-C-methylerythritol-4-phosphate (MEP) pathway (or non-mevalonate pathway) responsible for isoprenoid biosynthesis in a variety of bacteria, including *Francisella tularensis*. Since the MEP pathway has no homologs in the human genome, it is an attractive target for antibiotic development. IspD was cloned, expressed, and purified. An assay which could be adapted to high throughput screening was used to determine the  $K_M = 177.9 \pm 35.2 \mu\text{M}$ ,  $K_{\text{cat}} = 1.0 \pm 0.10 \text{ s}^{-1}$ , and  $K_{\text{cat}}/K_M = 3.4 \times 10^5 \pm 6.7 \times 10^4 \text{ M}^{-1} \text{ s}^{-1}$ . FtlspD was found to exclusively prefer  $\text{Mg}^{2+}$  for catalytic activity, and demonstrated the highest nucleotide specificity for CTP, although

deoxy-CTP, ATP, GTP, TTP, and UTP resulted in some enzymatic activity. Site directed mutants were used to probe whether the enzyme could be regulated by phosphorylation at a conserved T141 site. Bioprospecting was also evaluated as an alternative to costly high throughput screening, and although a ligand for IspD was not discovered in a tested natural product molecular library, the bioprospecting method was validated by isolating fosmidomycin from its known target, IspC.

## Introduction

*Francisella tularensis* is a facultative intracellular bacterial pathogen known for causing the debilitating and potentially fatal zoonotic disease Tularemia. Humans generally acquire it naturally by bites from infected insects, drinking tainted water, direct contact with infected animals, or by inhalation of aerosolized bacteria [1]. Like other bacterial infections, tularemia can manifest itself in various forms depending on the mode of exposure, such as ulceroglandular tularemia from skin exposure (the most common form), typhoidal (septicemic) tularemia which can occur as a secondary infection, and pneumonic tularemia from inhalation of *F. tularensis* which may accompany ulceroglandular and typhoidal infections or occur on its own. Pneumonic tularemia is the most threatening type of *F. tularensis* infection with a mortality rate as high as 30% in untreated cases, and develops in 10 - 15% of ulceroglandular cases and approximately 50% of typhoidal cases [2].

While incidents of naturally acquired tularemia have declined over the years, well-documented outbreaks have occurred that illustrate *F. tularensis*' ease of dissemination and virulence, the latest of which happened in 2000 at Martha's Vineyard

in Massachusetts, United States [3, 4]. In those outbreaks, it was determined that 11 of 15 confirmed tularemia cases were primary pneumonic tularemia [4], and the significant risk factors for confirmed cases included engaging in lawn mowing and brush cutting. This ease of dissemination displayed by *F. tularensis* made it a subject of interest to several militaries around the world that are alleged to have researched *F. tularensis* as a biological weapon throughout the 20<sup>th</sup> century [5]. The Centers for Disease Control (CDC) has recently assigned *F. tularensis* a Category A bioterrorism agent status to emphasize the high threat posed by an intentional release of the organism over a highly populated area, likely in an aerosolized form and consisting of genetically engineered, highly virulent, drug-resistant strains.

Genetically engineered and naturally acquired antibiotic resistance can complicate the threat posed by *F. tularensis*. Much attention is being given to the emergence of bacteria resistant to multiple drug classes [6] such as methicillin-resistant *Staphylococcus aureus* (MRSA) and the strains of *Mycobacterium tuberculosis* known as multidrug and extremely drug resistant (MDR-TB and XDR-TB, respectively). The increasing proliferation of drug-resistant bacteria and their ability to transfer resistance traits to other bacterial species makes it probable that *F. tularensis* could acquire resistance traits in its natural zoonotic hosts and reservoirs. Developing new drugs is an important component of preparing the healthcare system for highly drug-resistant infectious outbreaks, whether they are natural or manmade.

Isoprenoid biosynthesis has become an important target of study in pathogenic organisms because of their essentiality and ubiquity in biological systems. The isoprenoids are an expansive category of molecules that all derive from the repetitive condensation of two precursor molecules, which are isopentenyl diphosphate (IPP) and dimethylallyl diphosphate (DMAPP). The resulting molecules have wide and diverse functions such as sterols, structural components, pigments, cell signaling, and vitamins [7], thus cellular function is dependent on the ability to produce and regulate isoprenoid biosynthesis. IPP and DMAPP have been known to be synthesized via the classical mevalonate (MVA) pathway described in the 1950s [8] and was thought to be universal. The 2-C-methyl-D-erythritol 4-phosphate (MEP) pathway was detected and reported in the early 1990s [9] and is now known to be the primary pathway for producing IPP and DMAPP in many organisms. For almost all organisms the MVA and MEP pathways are exclusive. The MVA pathway is the sole producer of IPP and DMAPP in humans (all mammals), many Gram-positive bacteria, archaea, and fungi. Some notable bacteria use the MVA pathway, such as *S. aureus* and *Coxiella burnetii*, while a select few such as *Listeria monocytogenes* harbor genes encoding enzymes from both pathways [6]. All Gram-negative and some Gram-positive bacteria solely utilize the MEP pathway, including *F. tularensis* [10], *Mycobacterium tuberculosis* [11, 6], *Brucella abortus* [12], *Streptomyces coelicolor* [13], and *Escherichia coli* [14, 15]. The MEP pathway has also been shown to be the operative IPP biosynthesis pathway in the *Plasmodium* parasites that cause malaria, one of the most devastating human diseases in the world [16, 17]. In

the case of plants, which use both pathways simultaneously, the MVA and MEP pathways are compartmentalized in the cytosol and plastids, respectively, and each pathway contributes to different sets of isoprenoid categories with little overlap [18, 19]. However, there are no known convergent intermediate steps between the two pathways – each has a wholly separate set of enzymes and intermediates leading to the production of IPP and DMAPP.

The MVA pathway is illustrated in Figure 1, and the MEP pathway is illustrated in Figure 2.

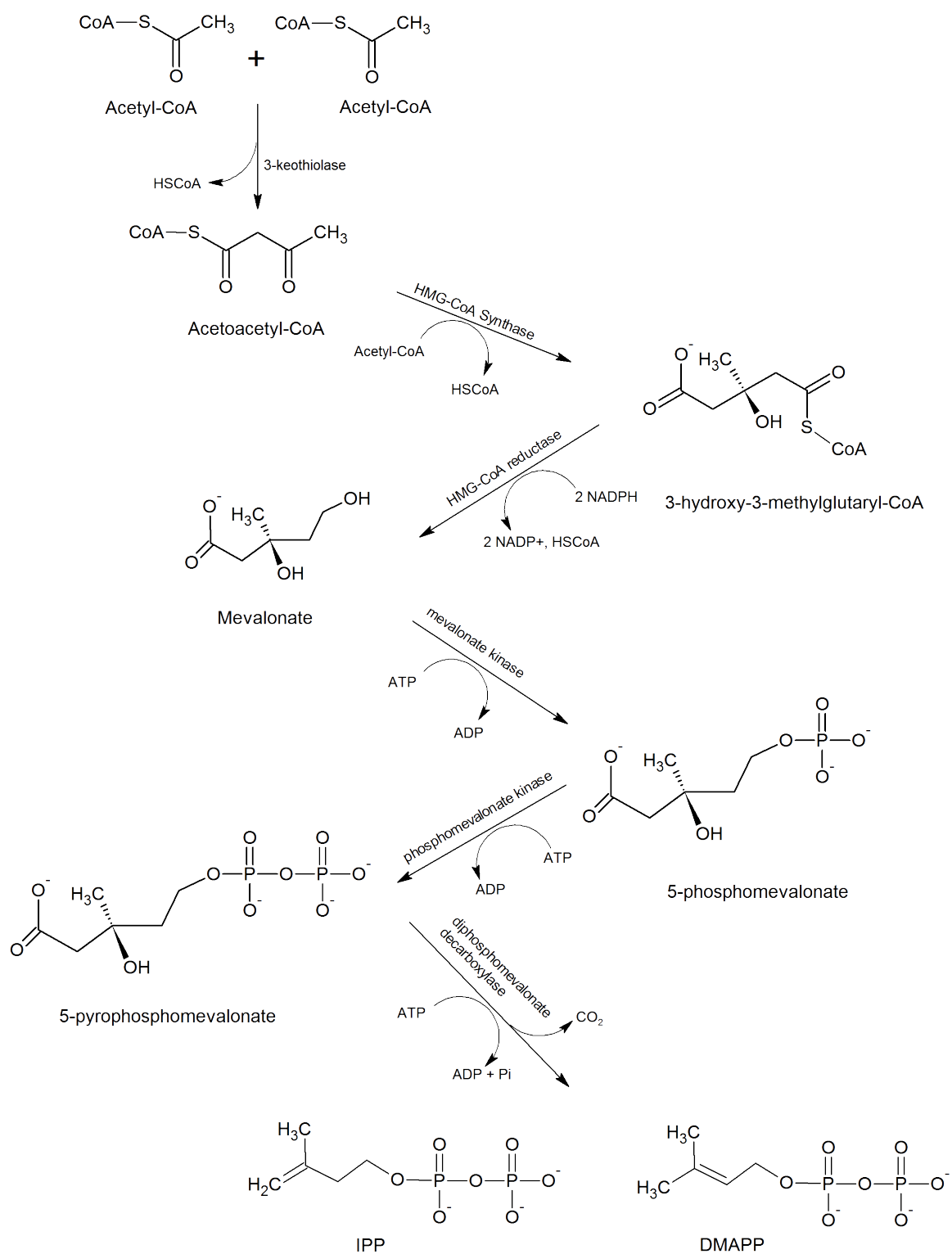
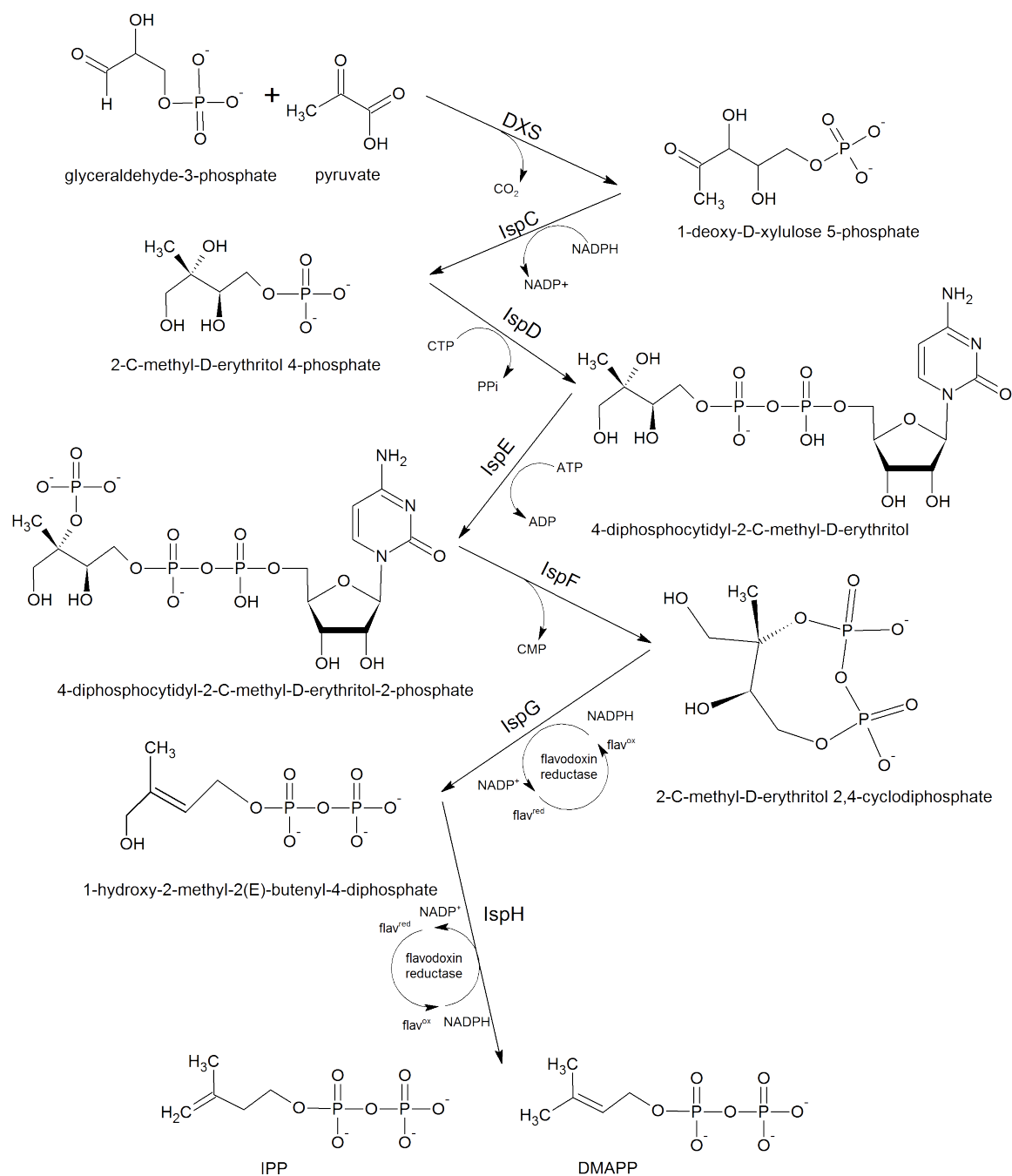


Figure 1 - Schematic of the MVA Pathway [6, 8]



**Figure 2 - Schematic of the MEP pathway [6].**



The MEP pathway consists of seven enzymatic steps as outlined in Figure 2. Glyceraldehyde-3-phosphate and pyruvate are condensed by DXP synthase (DXS) to 1-deoxy-D-xylulose-5-phosphate (DXP or DOXP). Next, IspC (DXP reductoisomerase or MEP synthase) converts it to 2-C-methyl-D-erythritol 4-phosphate (MEP). IspD (CDP-ME synthase or MEP-cytidylyltransferase) adds CTP to MEP to yield 4-diphosphocytidyl-2-C-methyl-D-erythritol (CDP-ME). IspE (CDP-ME kinase) phosphorylates CDP-ME at the C2 position of the methylerythritol moiety, giving CDP-ME2P, which is then cyclized by IspF (cMEPP synthase) to give 2-C-methyl-D-erythritol 2,4-cyclodiphosphate (cMEPP). IspG (HMBPP synthase) breaks the ring to give 1-hydroxy-2-methyl-2-(E)-butenyl-4-diphosphate (HMBPP), and IspH (HMBPP reductase) produces the isomers isopentenyl diphosphate (IPP) and dimethylallyl diphosphate (DMAPP) in a 5:1 ratio [6].

The exclusive use of the MVA pathway in humans and animals for isoprenoid biosynthesis makes the MEP pathway an attractive drug target for treating diseases caused by bacteria or parasites that rely on the MEP pathway for survival. The MEP pathway is vital for cellular survival as shown by transposon mutagenesis [10], where Gallagher *et al.* identified the genes essential for the survival of *F. novicida* by randomly disrupting its genome with antibiotic resistance trait inserts. Mutated cells grown on selective media were sequenced to identify the genes that could be disrupted without lethal effects, while disruption of essential genes presumably failed to produce viable cells. After ensuring complete insertion coverage of the *F. novicida* genome, no cells

containing insertions in any of the MEP pathway genes could be isolated, indicating that the loss of any step of the MEP pathway is lethal to the organism [10].

Fosmidomycin and FR-900098 are specific inhibitors of IspC that are lethal to the organism [6, 11, 20]. Fosmidomycin has been shown to be effective in combination with other antimalarial drugs for treating malaria patients by killing the parasite during its intraerythrocytic stages, although monotherapy in humans failed to provide a complete cure [17, 21]. A combination of fosmidomycin and clindamycin is currently in phase II clinical trials for the treatment of malaria [21].

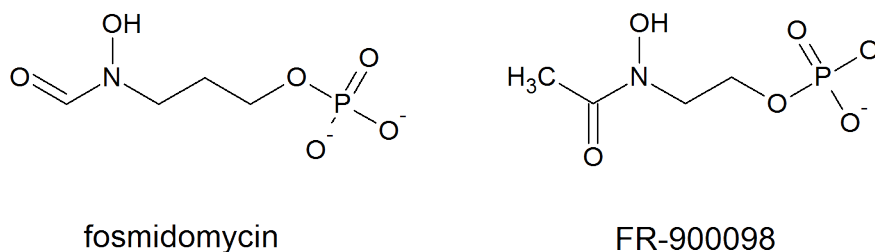


**Figure 3 - The IspC inhibitors fosmidomycin [21] and FR-900098 [38].**

Fosmidomycin has poor lipophilicity [17, 22], which makes it unlikely to diffuse into cells and require transport. Absorption into bacterial cells occurs by transport via the glycerol-3-phosphate transporter GlpT in *E. coli* and other bacteria, and it was shown that mutants deficient in GlpT were resistant to fosmidomycin [23]. Gram positive bacteria do not have GlpT, so uptake is especially poor in species such as *M. tuberculosis* and *M. smegmatis*, conferring resistance [11, 24]. The development of stable fosmidomycin resistance has also been demonstrated in *Plasmodium falciparum* [25].

IspC was discovered and identified as the target of fosmidomycin in 1998 (reviewed in [26]), and is perhaps the most studied enzyme of the MEP pathway because it is the first committed step. Isoprenoid biosynthesis is the only known function for MEP, while DXP can be used as a precursor for other metabolites such as pyrodoxol and thiamine [18]. Despite its limitations, fosmidomycin has facilitated the study of IspC as a target for improved therapeutics in *F. tularensis* [27]. IspC clones from *E. coli* [13, 14] have served as models for study of the pathway in bacteria.

IspD is the third overall step of the MEP pathway that catalyzes the cytidylation of MEP. It is also a target of interest because it is an early step in the pathway and could serve as a secondary target to counter resistance to IspC-targeted drugs. Interestingly, Zhang *et al.* determined recently that fosmidomycin is also a weak inhibitor of IspD. Their studies suggest that fosmidomycin works by inhibiting IspC halfway through its reaction, which renders it unable to fully convert DXP to MEP. The intermediate, 2-C-methylerythrose 4-phosphate, accumulates and subsequently competitively binds IspD along with fosmidomycin causing MEP to accumulate and the levels of metabolites downstream from IspD decrease. 2-C-methylerythrose 4-phosphate is likely to bind IspD with greater affinity than fosmidomycin due to a higher number of hydrogen bonds as shown by their docking studies. They measured fosmidomycin binding to IspD with  $IC_{50} = 20.4 \pm 3.3 \text{ mM}$  *in vitro*, an affinity  $10^4$  times weaker than the  $IC_{50} = 0.81 \pm 0.27 \text{ }\mu\text{M}$  measured for IspC [21].

The prospect of a drug with a dual inhibitory mechanism could lead to monotherapy regimens with the same efficacy of multidrug treatments and lower risk of

resistance development, because an organism is much less likely to develop multiple resistance traits simultaneously. Similarly, the development of a novel inhibitor of a downstream MEP pathway enzyme could lead to highly effective therapy in combination with fosmidomycin or provide protection against Gram positive bacteria. While other compounds have been reported to inhibit IspD (L-erythritol 4-phosphate,  $K_i = 240 \pm 17$  mM; and D-erythritol 4-phosphate,  $IC_{50} = 1.36$  mM) [12], these are quite weak relative to the inhibition constants of useful drugs like fosmidomycin, with  $K_i = 99$  nM,  $IC_{50} = 247$  nM for *F. tularensis* IspC [27]. The challenge in developing new effective MEP pathway inhibitors relies on optimizing for specificity, affinity, and delivery.

To date, IspE and IspF are the only MEP pathway enzymes for which inhibitor lead identification via a high throughput screen (HTS) have been published [28, 29]. The reactions can be measured by spectroscopic methods to expedite HTS processes [6]. IspG and IspH catalyze more complex reactions involving several redox cofactors or require anaerobic conditions that may severely limit the ability to perform fast analyses in a HTS system [6].

The drug development process consists of five general phases: target identification, target validation, lead molecule identification, lead molecule optimization, and preclinical and clinical trials. This project focused on characterizing and validating IspD in *F. tularensis* as a potential target for novel therapeutics. Enzyme kinetic parameters were measured, the amenability of IspD to high throughput screening was determined, a site of possible phosphoregulation was probed, and an alternative method

of bioprospecting for molecule leads by screening for molecules that bound to IspD was investigated.

Relatively few IspD homologs have been isolated and characterized. Studies have documented IspD from bacteria such as *E. coli* [14, 15, 30] and *M. tuberculosis* [31], while some reported the bifunctional IspDF enzyme found in organisms such as *Campylobacter jejuni* [32] and *Helicobacter pylori* [33] in which both proteins are encoded in the same transcription unit, forming a single enzyme with dual functionality. In *E. coli*, *M. tuberculosis*, and *F. tularensis*, the genes encoding IspD and IspF are in close proximity to each other on the bacterial chromosome, but are not expressed in a single unit. *F. tularensis* IspD has low homology with other species. For example, *E. coli* IspD has 34% homology, while *M. tuberculosis* IspD is only 25% similar. This project adds the characterization of *F. tularensis* IspD to the literature as a potential target for novel antibiotics.

## Experimental Aims

### Cloning, expression, and purification.

The gene encoding IspD in the *F. tularensis* subsp. *holarctica* LVS genome was cloned into a bacterial plasmid vector and overexpressed in a standard laboratory strain of *E. coli* so that sufficient quantities of the purified protein (FtIspD) could be obtained for study. *E. coli* IspD (EcIspD) was also cloned and used as a control for the FtIspD data. This allowed validation of the data obtained to reported values of EcIspD. The protein was then purified for downstream experiments.

### Assays

IspD enzymatic activity was quantified using a spectrophotometric assay adapted from Bernal *et al* [30]. This characterization allowed for analytical comparison of protein activity levels that might be observed during molecular library and lead compound candidate testing.

IspD's *in vitro* substrate affinity was determined, as well as its preferences for divalent metal cations and nucleotides. The assay was also adapted to a high throughput screen in a microtitre plate. CaCl<sub>2</sub>, an inhibitor of pyrophosphatase (not IspD), was used

to simulate an inhibited assay which might be observed in the event of a hit during a high throughput screen, through which the robustness of the assay could be evaluated using the Z-factor.

### **Regulation of IspD**

Phosphorylation of amino acid sites is a widely used intracellular mechanism for signal transduction and regulating the activities of enzymes. The goal here was to identify amino acid residues that might play a role in the regulation of IspD *in vivo*. Because the FtIspD structure has not yet been solved, a model was constructed to show the probable locations of phosphorylation sites on the protein. Phosphopeptide fragments were then identified via LC-tandem-mass spectrometry by Dr. Weidong Zhou of the Center for Applied Proteomics and Molecular Medicine at George Mason University.

After finding the T141 residue to be conserved, phosphorylated, and located in a structurally significant location of the protein model, the mutants T141D and T141E were cloned, expressed, purified, and assayed for activity. Intrinsic fluorescence studies of wild type and mutant IspD were then performed to see if any changes in folding or structure resulted from the site mutations. Ms. Amy Fisher (Center for Nanophotonics Imaging, George Mason University) helped immensely with this work.

### **Bioprospecting**

An alternative method for identifying lead molecules in a molecular library was investigated as part of this study. In this bioprospecting study, the protein of interest was

immobilized on a purification column. A molecular library was then passed over the protein, unbound material washed out, the protein eluted, and binding molecules were separated from the protein and analyzed by LCMS to aid in identifying them. This approach could expedite inhibitor lead identification and prove to be a viable lower cost alternative to high throughput screening by selecting for molecules that bind to the protein. Bound molecules would be subsequently identified.



## Materials and Methods

### Cloning

The gene encoding IspD (YP\_514172) in the *F. tularensis* subsp. *holarctica* LVS genome (accession number NC\_007880) was cloned into a pET101/D – TOPO plasmid (Invitrogen). The gene was constructed with a C-terminal His tag and amplified via PCR as described in [35]. The plasmid was transformed into BL21 (DE3) CodonPlus-RIL competent cells (Stratagene) for overexpression and cells were grown in LB media (Fisher) with 100 µg/mL ampicillin and 50 µg/mL chloramphenicol. Expression was induced with 0.5mM IPTG.

The *E. coli* ispD gene (NC\_000913.2: 2869802..2870512) encoding the respective enzyme (NP\_417227) was cloned into a pET28c plasmid (EMD) with a N-terminal His tag similar to *E. coli* IspD constructs used in the literature [15, 30]. *E. coli* K12 genomic DNA (NC\_000913) was used in the PCR process. PCR primer pairs flanking the IspD gene consisted of:

Forward: 5'-AAAAACATATGATGGCAACCACTCATTG-3'.

Reverse: 5'-GGGGTCCTCGAGTTATGTATTCTCCTG-3'.

*E. coli* K12 genomic DNA was obtained by using a GenElute Miniprep Kit (Sigma). The PCR was set up using 25  $\mu$ L 2x Phusion HF, 2.5  $\mu$ L each forward (44.2  $\mu$ M) and reverse (39.1  $\mu$ M) primers, 3  $\mu$ L genomic DNA, and 17  $\mu$ L ddH<sub>2</sub>O covered with 50  $\mu$ L mineral oil. The PCR reaction consisted of heating to 98°C for 30 seconds, 62°C for 30 seconds, and 72°C for 90 seconds for 24 cycles, then held at 72°C for 10 minutes and finally kept at 4°C until use. The PCR product was purified using the Sigma GenElute PCR Cleanup Kit and ligated into the pET28c plasmid vector (Novagen) using Lyo-Ligase and the Xho I and Nde I restriction sites. The plasmid was then transformed into Novagen Blue Singles cells with a 30 second heat shock at 42°C. These cells were grown in LB media with 50  $\mu$ g/mL kanamycin to select for cells that contained the plasmid. Cultures were grown on LB agar and colonies containing the correct plasmid and gene insert were selected using restriction mapping. The fragments were visualized via agarose gel to verify the plasmid's integrity. After verification of the proper size fragments, the plasmid containing the IspD insert (pEcIspD) was sequenced.

pEcIspD was transformed into chemically competent Stratagene *E. coli* BL21 (DE3) codon+ cells for expression. Transformation was performed by incubating competent cells with DNA at 4°C for 30 minutes, 30 seconds heat shock at 42°C, 4°C for 2 minutes, addition of 250  $\mu$ L SOC media broth to the vial, and then incubated and shaken for 1 hour at 37°C, 250 RPM. The successful competent cells were kept in storage at -80°C in 20% glycerol.

## Protein Expression and Purification

A 10 mL seed culture was grown at 37°C with shaking at 250 RPM, with *E. coli* BL21 CodonPlus (DE3)-RIL cells containing pFtlspD. After 18 hours, the culture was used to inoculate one liter of fresh LB media, grown to an OD<sub>600</sub> of 1.1 and induced with 0.5 mM isopropyl-β-D-1-thiogalactopyranoside (IPTG). The production flask was incubated for 18 hours at 37°C, 250 RPM, and the cells were harvested by centrifugation at 19,200g, 4°C and stored at -80°C until use.

Cell pellets were lysed with “Buffer A” containing 0.1 M Tris pH 8.0, 0.1 M NaCl, and 0.032% (w/v) lysozyme. 3 ml of this buffer per gram of cell pellet was used. “Buffer B” (0.1 M CaCl<sub>2</sub>, 0.1 M MgCl<sub>2</sub>, 0.1 M NaCl, 0.02% DNase, 0.3 mL per gram pellet) was added after. The lysate was centrifuged at 48,000g for 30 minutes at 4°C. The clarified lysate was then passed over Talon superflow resin with immobilized Co<sup>2+</sup> to capture the protein via the His-tag. It was washed with 20 column volumes of the equilibration buffer (50 mM HEPES pH 7.5, 300 mM NaCl), 20 column volumes of wash buffer (50 mM HEPES pH 7.5, 300 mM NaCl, 10 mM imidazole), and eluted with 10 column volumes of elution buffer (50 mM HEPES pH 7.5, 300 mM NaCl, 150 mM imidazole). The protein was buffer exchanged into 0.1 M Tris pH 8.0, 1 mM NaCl, snap-frozen and stored at -80°C. The typical yield of IspD was 15 mg of IspD per 1 liter culture with high purity as visualized by SDS-PAGE and coomassie staining.

## Enzyme Assays

IspD activity at 37°C was determined by measuring the production of pyrophosphate (PPi) in solution as described by Bernal *et al* [30].

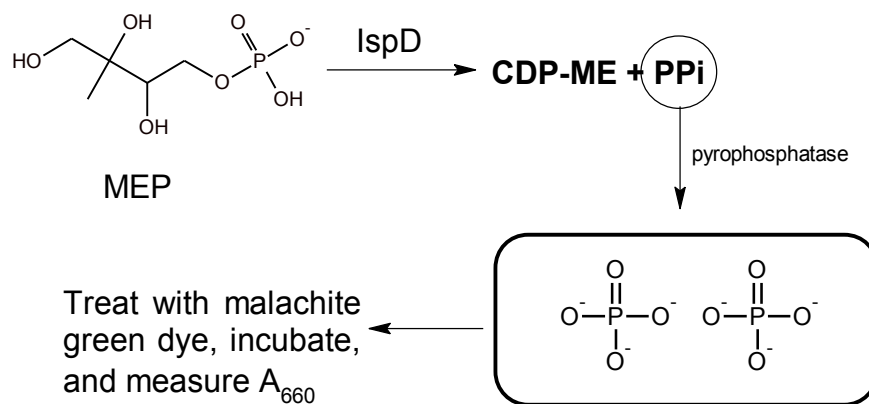


Figure 4 - Schematic of the IspD assay.

The dye stock contained 0.44 g malachite green in 360 mL of 3M  $\text{H}_2\text{SO}_4$  and was stored at 4°C. A working stock of dye was made prior to each assay by mixing 2.5 mL of the malachite green stock, 0.625 mL of 7.5% (w/v) ammonium molybdate, and 50  $\mu\text{L}$  Tween 20.

For evaluating the MEP-dependent kinetic activity of IspD, a reaction mix was made containing 100 mM Tris pH 8.0, 1 mM  $\text{MgCl}_2$ , 1 mM dithiothreitol (DTT), 0.2 mM cytidine 5'-triphosphate (CTP), 100 mU/mL pyrophosphatase, 75  $\mu\text{g/mL}$  IspD, and varying concentrations of MEP. The reaction mixture was incubated at 37°C, a 40  $\mu\text{L}$  aliquot was drawn every 30 seconds, added to 120  $\mu\text{L}$  of water and 40  $\mu\text{L}$  of the dye reagent. After incubating this mixture for 10 minutes at 37°C, 22  $\mu\text{L}$  of 34% sodium

citrate was added to the assay solution and incubated for 30 minutes at 37°C. The  $A_{660}$  of this assay solution was recorded and used to determine the concentration of pyrophosphate produced from a standard curve.

Data were fit by nonlinear regression to the Michaelis-Menten equation (below) to determine the  $V_{\max}$ ,  $K_m$ ,  $K_{\text{cat}}$  and  $K_{\text{cat}}/K_m$  for MEP and CTP substrates, where  $Y$  corresponds to the velocity of the reaction and  $X$  represents the substrate concentration.

$$Y = \frac{V_{\max} * X}{(K_m + X)}$$

For the high throughput assay, the volume of the reaction was scaled from 1 mL to 200  $\mu\text{L}$  and 1 mM  $\text{CaCl}_2$ , a complete inhibitor of pyrophosphatase [37], was used as a control for assay inhibition visualization.

Metal ion specificity was determined among  $\text{Mg}^{2+}$ ,  $\text{Ca}^{2+}$ ,  $\text{Mn}^{2+}$ ,  $\text{Co}^{2+}$ ,  $\text{Cu}^{2+}$ , and  $\text{Zn}^{2+}$ . After incubating IspD with the reaction mixture containing the variable metal cation (pyrophosphatase excluded), EDTA was added to chelate divalent cations so that it would not interfere with pyrophosphatase activity, which is dependent on  $\text{Mg}^{2+}$ . The reaction was filtered through a Millipore Microcon 10K MWCO filter to remove IspD and pyrophosphatase was added to the reaction mixture. The solution was dyed, and the  $A_{660}$  was read as normal.

The Z-factor, a statistical indicator of signal error in an assay, was calculated as described by Zhang et al [36]. This parameter is determined by the equation:

$$Z = 1 - \frac{(3\sigma_s + 3\sigma_c)}{|\mu_s - \mu_c|}$$

where  $\sigma$  is the standard deviation of the sample (s) or control (c), and  $\mu$  is the mean of the sample or control, respectively.

### **Size Exclusion Chromatography**

The molecular mass of IspD and mutants were determined using size exclusion chromatography on a sephacryl 200 column (Sigma) and measured with a gel filtration protein standard (BioRad 151-1901). The mobile phase contained 0.1M tris pH 8.0, 1 mM NaCl at 2 mL/min at room temperature (22°C). A 100  $\mu$ L load sample was used containing protein at 8.9 mg/mL. The sample was centrifuged at 16,110g rpm for 10 minutes prior to loading.

### **Phosphopeptide Analysis**

IspD expression was induced with 0.01 mM IPTG (instead of the normal 0.5 mM). After purification, the enzyme was reduced with 10mM DTT, alkylated by 50 mM iodoacetamide, and digested with trypsin (Promega) in ammonium bicarbonate buffer (50 mM, pH 9.0), and urea (2 M). The mixture was desalted using a SepPak column (Waters, Milford, MA). A TiO<sub>2</sub> column was used to separate phosphopeptides from the digestion mixture and the phosphopeptides were analyzed via reverse-phase liquid chromatography nanospray tandem mass spectrometry (LC-MS/MS) with an LTQ-Orbitrap mass spectrometer (ThermoFisher). SEQUEST was used to identify phosphopeptides.

## **Mutagenesis**

T141D and T141E mutants were cloned by GenScript Corporation and expressed in Stratagene *E. coli* BL21 CodonPlus (DE3)-RIL cells. Expression, purification and assays were performed as described for wild type IspD.

## **Fluorescence Spectroscopy**

The intrinsic fluorescence was measured with a Fluoromax-3 fluorometer (Horiba Jobin Yvon) using a 5  $\mu$ M protein concentration against a buffer blank (0.1 M Tris pH 8.0, 1 mM NaCl). An excitation wavelength of 290 nm was emitted and emissions were measured between 310-400 nm using a 5 nm slit.

## **Molecular Modeling**

Sequences containing phosphorylated residues were identified and mapped onto a structural model of FtIspD built with the I-TASSER server. Model quality was assessed using ProQRes on the ExPASy server. Models were viewed and edited using the Deep View, and graphics were generated in PyMOL.

## **Bioprospecting**

A model library made using V8 vegetable juice was filtered through a 3000 MWCO filter to remove macromolecules and particulates. The filtrate was centrifuged and the supernatant was passed over immobilized IspD protein on a TALON column as an extra step in the purification protocol. It was washed with the equilibration and wash buffers, and the protein was eluted with the elution buffer.

The eluate was heated at 75°C for 10 minutes to denature the enzyme and filtered through a 3000 MWCO filter to remove IspD. The filtrate was analyzed via LCMS on a Waters Micromass ZQ liquid chromatography system with quadrupole detector with electrospray ionization. The same procedure was applied to IspC using fosmidomycin. Analysis of fosmidomycin standards was performed on the LCMS with a reverse phase C18 column using a 0-50% acetonitrile gradient over 30 minutes and ionized using the following parameters: ESI negative, capillary 4.0 kV, cone: 18V, source temperature 150°C, desolvation 250°C, 250 L/hr, with the data published in [38] as a starting point.



## Results and Discussion

The need for novel antibiotics has grown due to the extensive spread of natural and engineered bacterial resistance to current drugs. Many pathogenic bacteria are known to solely utilize the MEP pathway for isoprenoid biosynthesis, which humans do not use, thus making it a highly attractive target. Although fosmidomycin is currently considered an effective inhibitor of the MEP pathway, resistance by way of limited uptake was identified early in its history [23]. However, no evidence has been found in the literature that mechanistic resistance to fosmidomycin caused by mutation of IspC in target organisms is responsible for resistance. Other commonly used antibiotics presently used in the treatment of *F. tularensis* infections are seeing increasing resistance in the world as well.

*Francisella tularensis* IspD is a 229 amino acid protein with a calculated molecular mass of 25.9 kDa encoded by the gene *ispD* (also known as *ygbP*). Recombinant FtIspD expressed with high copy number in the laboratory *E. coli* host with IPTG induction and was isolated with the polyhistidine tag with more than 90% purity. SDS-PAGE visualization shows the high purity after coomassie blue staining (Figure 7).

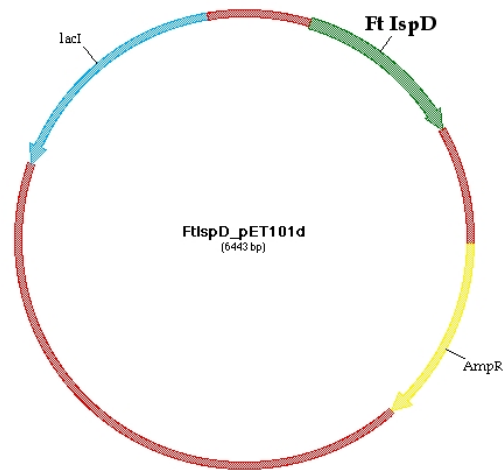


**Figure 5 - *F. tularensis* IspD in pET101 directional vector with topoisomerase (Invitrogen). The open reading frames for the ampicillin resistance gene and lac operon are also shown indicated as arrows**

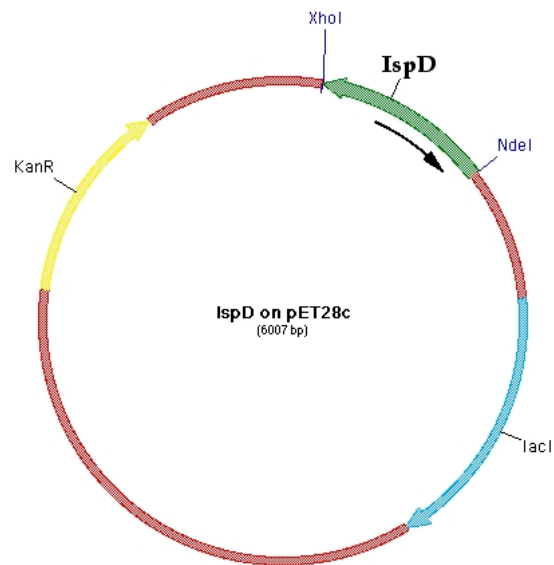


**Figure 6 - Vector map showing *E. coli* IspD in pET28c (pEc-IspD). The arrow beneath the IspD open reading frame indicates the IspF open reading frame on the complementary strand.**

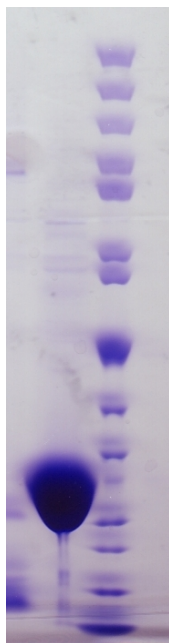


**Figure 7 - FtlIspD visualized by SDS-PAGE. The most intense band corresponds to a molecular mass of approximately 26 kDa with yield in excess of 15 mg purified protein.**

### **Kinetic Assay Results**

For the kinetic curves shown in Figure 8, assays were carried out at MEP concentrations ranging from 10 – 400  $\mu\text{M}$  while the CTP concentration was held at a saturating concentration of 200  $\mu\text{M}$  for the kinetic characterization. The activity of IspD was measured over a range of CTP concentrations from 10 – 400  $\mu\text{M}$  at a constant saturating MEP concentration of 200  $\mu\text{M}$ .

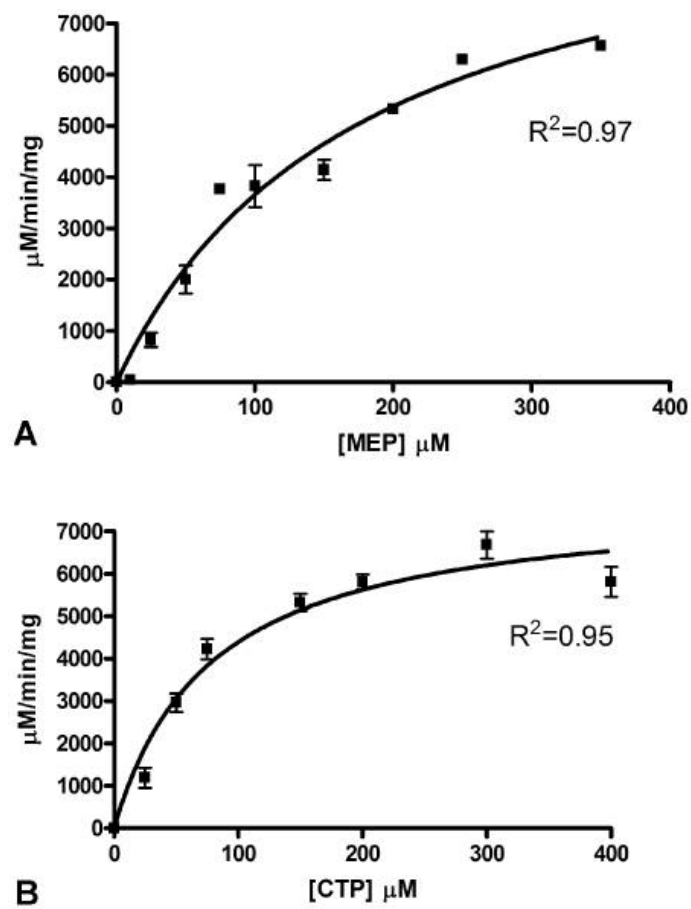


Figure 8 - *F. tularensis* IspD kinetic activity.\*

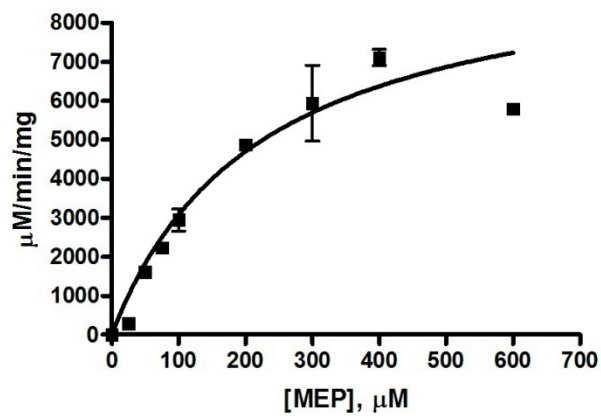


Figure 9 - *E. coli* IspD kinetic assay, MEP dependent.

**Table 1 - MEP cytidyltransferase Apparent Kinetic Parameters. N/A entries were not determined.**

<i>MEP cytidyltransferase</i>	$K_M^{MEP}$ ( $\mu M$ )	$K_M^{CTP}$ ( $\mu M$ )	$k_{cat}^{MEP}$ ( $s^{-1}$ )	$k_{cat}^{CTP}$ ( $s^{-1}$ )	$k_{cat}^{MEP} / K_M^{MEP}$ ( $M^{-1} min^{-1}$ )	Source
<i>F. tularensis</i>	177.9	73.0	1.0	0.8	$3.4 \times 10^5$	[35]
<i>E. coli</i> (test clone)	221.9	N/A	57.1	N/A	$1.5 \times 10^7$	Exp Data
<i>E. coli</i>	61	58	0.7	54.1	$6.6 \times 10^5$	[30]
range of kinetic parameters from two sources	370	760	25.9	N/A	$7.86 \times 10^6$	[15]

The observed kinetic values for FtIspD were  $K_{cat}^{MEP} = 1.0 \pm 0.10 s^{-1}$  and  $K_{cat}^{MEP} / K_M^{MEP} = 3.4 \times 10^5 \pm 6.7 \times 10^4 M^{-1} s^{-1}$  (Table 1). The *F. tularensis* data in this study were measured with the colorimetric assay and are comparable to the literature datasets, accommodating for differences in kinetics due to potential structural variations arising from the low sequence homology that FtIspD has to most other homologs. The kinetic values for EcIspD control in Table 1 are within the spread of literature values, although the malachite green assay indicated a  $K_M^{MEP}$  nearly four times higher for the in-house control clone than its literature counterparts. Bernal *et al.* obtained  $K_M^{MEP} = 61 \pm 14 \mu M$  [30] for *E. coli* via the malachite green assay, while radiological assays from other sources found the  $K_M^{MEP}$  ranging between a similar value of 32  $\mu M$  [13], and 370  $\mu M$  [15] all for the same enzyme. This wide spread of values may be attributed to the sensitivity of

the assays to handling or construct variations. Bernal *et al.* also suggest pyrophosphatase grade and condition may play a role in assay quality [30]. Regardless, the assay behaved predictably, and showed a strong measure of robustness with a high Z-factor of 0.8. Values over 0.5 are indicative of a robust assay for high throughput screening that has good signal response and low background interference [36]. This assay was scaled for a 96-well plate with MEP concentration increasing by row in Figure 10 from 0  $\mu$ M to 100  $\mu$ M. Columns 1-3 are replicate uninhibited assays, and columns 4-6 are replicate assays containing 1 mM  $\text{CaCl}_2$ , simulating an inhibitor candidate hit.

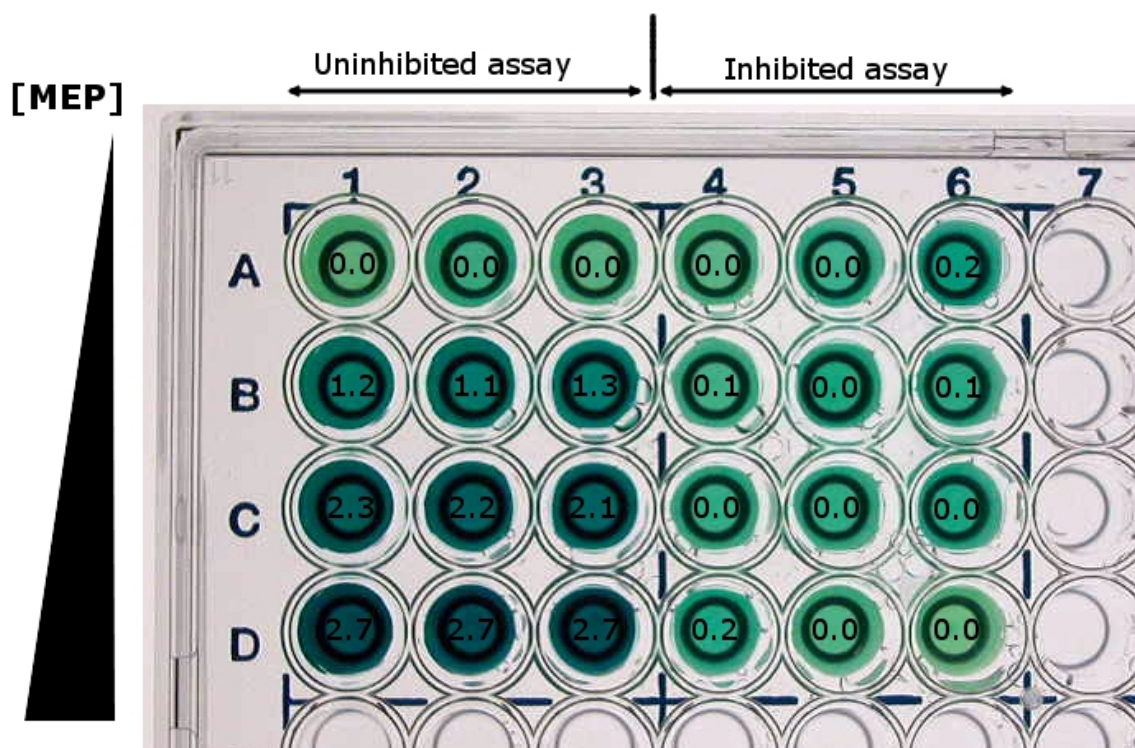


**Figure 10 - The robustness of the IspD assay can be visually perceived by this microtitre test. The absorbance value of each well is shown. Rows A-D contain 0, 25, 50, and 100  $\mu$ M MEP respectively, while columns 4-6 have  $\text{CaCl}_2$  added to them.**

## Metal Ion Preference

IspD's metal ion specificity was evaluated among  $\text{MgCl}_2$ ,  $\text{CaCl}_2$ ,  $\text{MnCl}_2$ ,  $\text{CoCl}_2$ ,  $\text{CuCl}_2$ , and  $\text{ZnCl}_2$ . The reaction was performed as usual except that EDTA was added after incubating IspD with substrate, the solution was filtered to remove IspD, and pyrophosphatase was then added to the filtrate to continue the assay as normal. Like other IspD homologs, FtIspD natively prefers  $\text{Mg}^{2+}$  to catalyze the reaction (Fig. 14).  $\text{Mg}^{2+}$  is essential for cytidyltransferase activity and is believed to aid in coordinating the phosphate groups of CTP and providing them complementary charge so that MEP can be cytidylated, displacing the PPi group [39].

During this experiment,  $\text{Mg}^{2+}$  was replaced with an alternative divalent metal chloride salt in the assay. Only  $\text{Mg}^{2+}$  supported assay activity with FtIspD, which contrasts from other studies on the *E. coli* and *M. tuberculosis* homologs that supported activity with at least one other divalent cation besides  $\text{Mg}^{2+}$ .

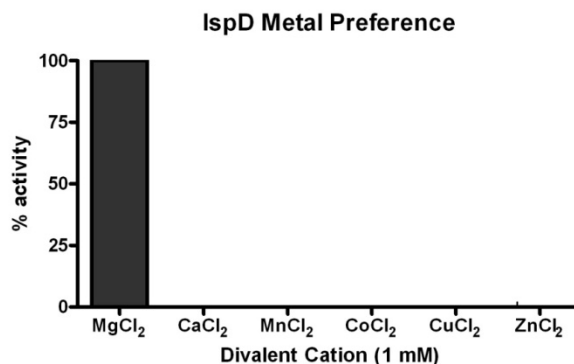


Figure 11 -  $\text{MgCl}_2$  was the only divalent metal salt tested that conferred measurable activity to FtIspD.

*E. coli* IspD was found to be catalytically active in the presence of  $Mg^{2+}$ ,  $Mn^{2+}$ , and  $Co^{2+}$  using a  $^{32}PPi$  liquid scintillation spectrometry assay [14]. Eoh *et al.*, also using the  $^{32}PPi$  assay, reported that *M. tuberculosis* IspD maintained comparable activity with  $Mn^{2+}$ , lower activity with  $Zn^{2+}$ , and  $Ca^{2+}$  was ineffective [31]. Shi *et al.*, using the coupled pyrophosphatase assay, detected activity in the same enzyme with  $Mg^{2+}$ ,  $Mn^{2+}$ ,  $Fe^{2+}$ , and  $Co^{2+}$ , while  $Zn^{2+}$  was ineffective [40]. Despite the difficulty in directly comparing these sets of data, the various studies agree overall that there is a clear specificity for  $Mg^{2+}$  and it is the preferential cation for IspD. There is significant interplay between the enzyme active site residues,  $Mg^{2+}$ , substrates, and solvent [39], and the arrangement of these components in FtIspD appears to be especially sensitive to the nature of the divalent cation in this study.

### **Nucleotide Specificity**

The activity of IspD in the presence of various nucleotides was measured at 200  $\mu M$  and 400  $\mu M$ . FtIspD displayed optimal activity with CTP as expected, while much lower levels of activity were detected in the presence of deoxy-CTP (dCTP), ATP, GTP, TTP, and UTP (Fig. 15). These results are consistent with the data reported for homologous enzymes. A 400  $\mu M$  concentration of nucleotide appeared to support higher relative activity in all nucleotides than 200  $\mu M$ , but at most only approximately one third of the activity demonstrated with CTP, indicating that FtIspD is very specific for CTP.



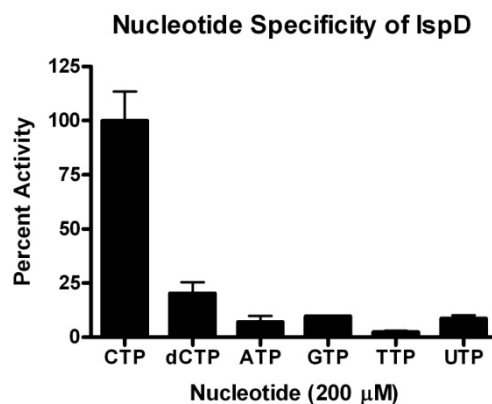


Figure 12 - IspD activity was greatest with CTP, and significantly less active with other nucleotides.

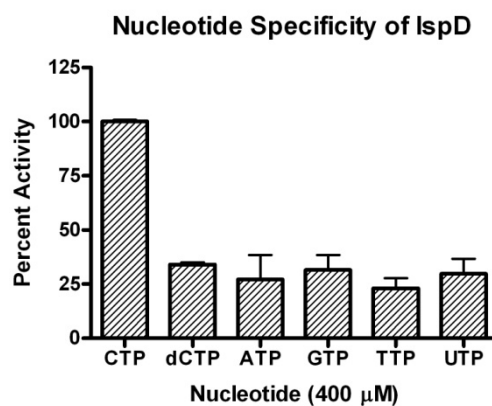


Figure 13 - At 400  $\mu$ M, the relative amount of activity increased slightly for other nucleotides, but was still much lower than activity with CTP, showing a clear preference.

## Phosphoregulation

The IspD active site involves a number of key residues that form a complex network with CTP,  $Mg^{2+}$ , and MEP in order to catalyze the reaction. In the EcIspD crystal structure, residues Asp106, Arg109, Thr165, and Lys213 form polar contacts with the MEP-derived moiety of CDP-ME within the active site cleft. Thr140' and Arg157' are contributed from the other chain in the dimer and also contact the MEP moiety of CDP-ME near the interface of the  $\beta$  arm domains, suggesting they may help guide MEP into the active site [39]. These residues are well conserved in FtIspD, as can be seen in Table 2. In the FtIspD model, these conserved residues all line the active site cleft and are expected to play similar roles. Regulation of IspD may occur through phosphorylation of one or more of these key residues. LCMS/MS analysis of FtIspD for phosphorylated amino acids indicated a phosphorylated threonine corresponding to the 141 position in the enzyme sequence. A sequence alignment showed that Thr141 in FtIspD is equivalent to Thr140 in EcIspD, and Richard *et al* predicted that this residue plays a key role in guiding MEP toward the active site for cytidylation during the reaction [39].

**Table 2 – Conserved active site residues in *E. coli* IspD [39] and *F. tularensis* IspD.**

<u>EclspD</u>	<u>FtlspD</u>
P13	P9
A15	A11
G16	G12
F17	I13
R19	T15
R20	R16
K27	K23
G82	G79
D83	E80
R85	R82
S88	S85
D106	D106
R109	R109
T165	T164
K213	K214
T140'	T141'
R157'	R156'

A homology model of FtlspD was constructed from the amino acid sequence using the iTASSER server [41, 42] in order to visualize the location of T141 in FtlspD. iTASSER constructs protein models by selecting templates for threading from the RCSB PDB database through identification of proteins with similar fold and super-secondary structures predicted by the sequence. Continuous fragments from the templates are then computationally assembled while unaligned regions (such as loops) are built by ab initio modeling. iTASSER constructed the enzyme model by building from several templates which included the *E. coli* crystal structures with PDB numbers 1I52 and 1INI. The

model output was then analyzed with ProQRes which rates the quality of each residue prediction as a score ranging from 0 (unreliable) to 1 (reliable) by measuring structural features within a sliding window including atom-atom contacts, residue-residue contacts, solvent accessibility surfaces, and secondary structure information [43].

As shown in Figure 15, the predicted fold of FtIspD strongly resembles EcIspD. Regions that were scored unreliable (below 0.5) by ProQRes are colored in green. Not surprisingly, this corresponds to a large swath of the small flexible  $\beta$  arm which would likely have poor structural predictability. Thr141 (highlighted in blue) lines up in a manner similar to Thr140 in the *E. coli* enzyme in the dimer, essentially at the entrance to the active site cleft.

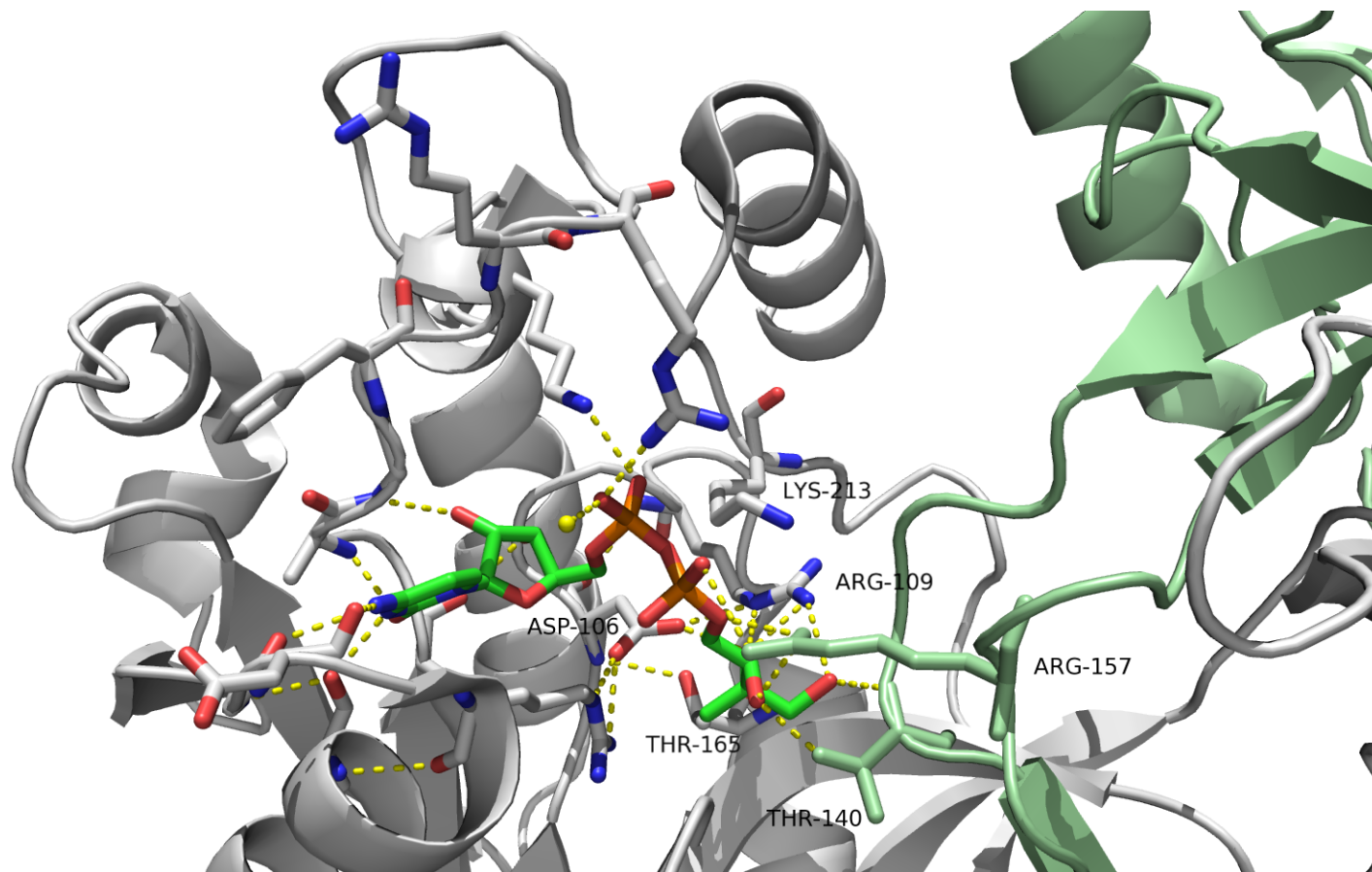


**Figure 14 - The active site network of *E. coli* IspD with the residues that contribute to the cytidylation of MEP labeled [39]. All of the labeled residues are highly conserved in *F. tularensis* IspD.**

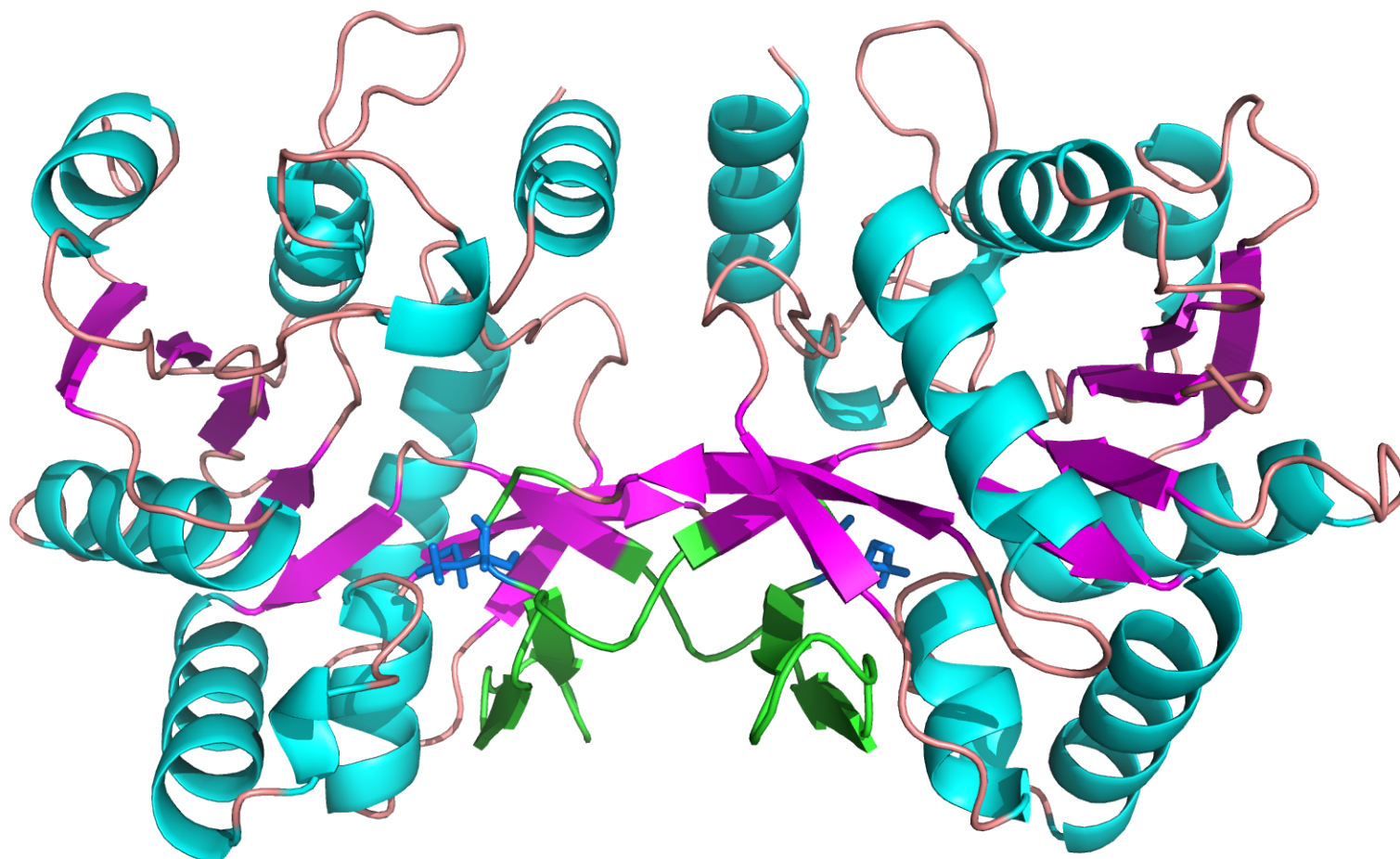


**Figure 15 - FtlSpD model predicted by iTASSER. The region in green scored below 0.5 in ProQRes. Thr141 is shown in stick form and colored dark blue.**

To determine if phosphorylation of Thr141 could play a role in inhibiting FtIspD and act as a regulatory mechanism, two mutants with Thr141 replaced by Asp (T141D) and Glu (T141E) were constructed to simulate a phosphate group attached to the residue. The wild type and mutant enzyme quaternary states were determined to be dimers using size exclusion chromatography (Figure 16). Assays of the enzymes showed that the T141D mutant lost approximately 75% of activity, while T141E lost all activity, indicating that Thr141 plays a crucial role in the reaction, and FtIspD would likely be inhibited by phosphorylation. There was also no shift in intrinsic fluorescence (Figure 18), indicating that there was no major conformational change between wild type active IspD and the T141D and T141E mutants. This suggests that the loss of activity is due to mechanistic blockage at the reaction site, not a loss of enzyme conformation.

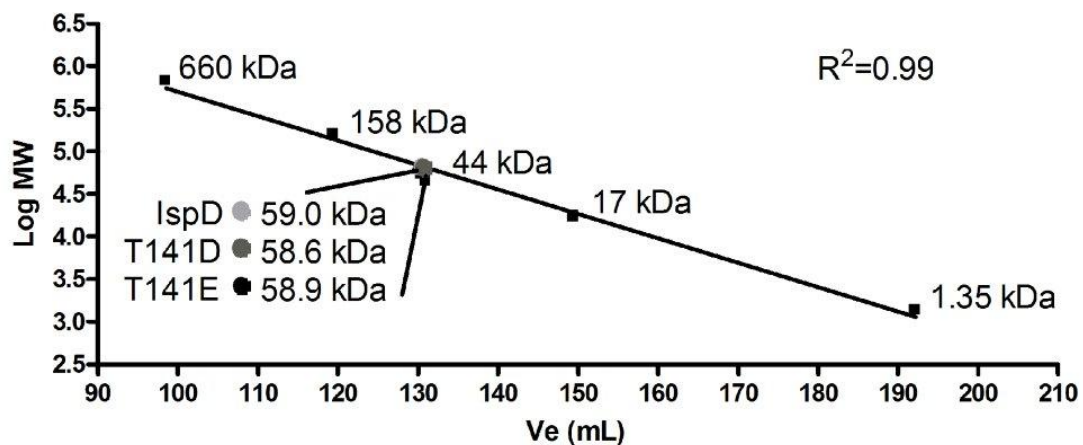
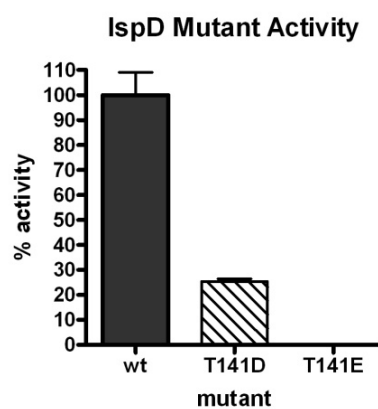
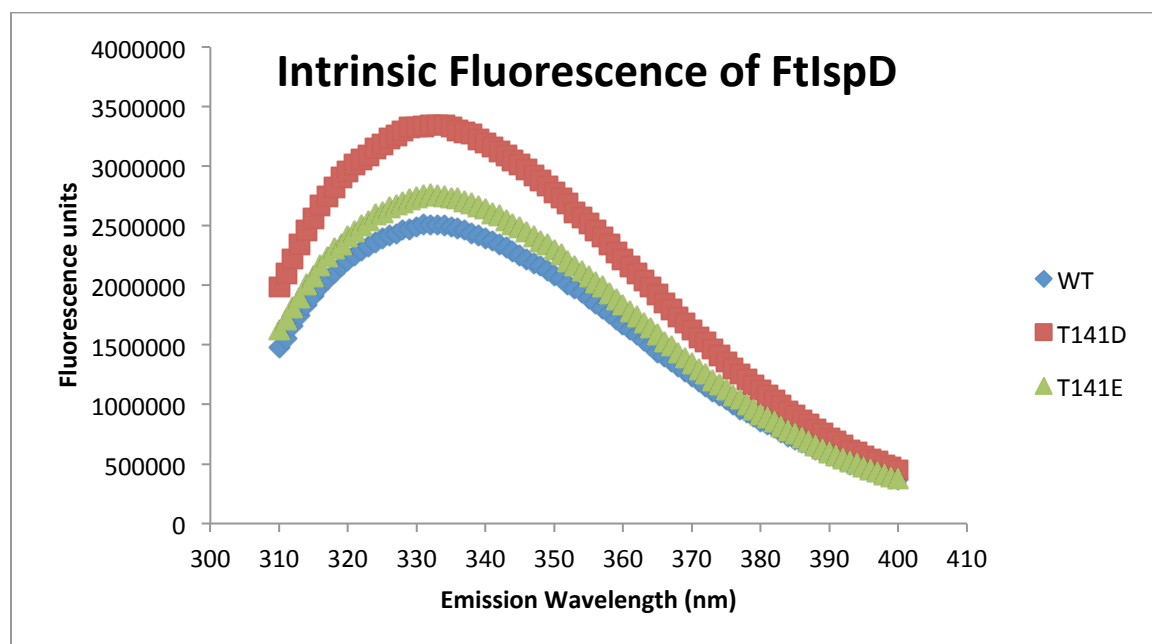


Figure 16 - Molecular masses of IspD wild type, T141D, and T141E mutants on a standard curve determined by size exclusion chromatography.



**Figure 17 -** Mutants constructed to simulate phosphorylation at the T141 site demonstrated markedly reduced activity, suggesting a T141 may be a site of regulation.



**Figure 18 -** Fluorescence of wild type and mutant IspD indicated no conformational changes of the enzyme after residue modification.



## **Bioprospecting**

An alternative approach to high throughput screening for lead molecule identification is bioprospecting, a process in which molecules that bind the target enzyme such as IspD would be separated from a mixture by their interaction with the enzyme. Traditional high throughput screening is a very resource intensive process and works essentially through brute force, by screening many thousands of purified compounds within molecular libraries and assaying the enzyme for each compound. In contrast, bioprospecting could be applied to mixed molecular libraries, such as raw extracts. This could allow much more rapid collection of molecular libraries without the need to identify and purify each compound within. In this case, the target protein is immobilized on a substrate, the molecular mixture is passed over it, washed, and the bound enzyme is analyzed for ligands.

To illustrate the use of bioprospecting as an alternative to an HTS for developing inhibitors of the MEP pathway, a proof of concept was established using IspC and its known inhibitor, fosmidomycin. Approximately 5 mg of IspC was immobilized on Talon cobalt resin via its polyhistidine tag following cell lysis, washed, and a solution of 200  $\mu\text{g/mL}$  fosmidomycin in water was passed over it. After elution, denaturation of the protein by heat, and filtration to separate it, the filtrate was compared to a fosmidomycin standard curve via LCMS in ESI negative mode. Ion peaks corresponding to fosmidomycin were identified (a molecular ion of 182  $m/z$  and a daughter peak of 136  $m/z$ ). The LCMS standard curve was calibrated to detect fosmidomycin concentrations

from 0.05 µg/ml to 7.5 µg/ml, and fosmidomycin was detected in highly diluted (1:1000) eluate at a concentration of 0.16 µg/ml, which shows that most of the fosmidomycin was recovered.

To screen for natural product inhibitors of IspD, a molecular library was constructed by filtering V8 juice (a product of concentrate from vegetable extracts suspended in tomato juice) through a 3000 MWCO filter and centrifuging the filtrate, then passing the supernatant over immobilized IspD as described for IspC above. While IspD displayed slightly inhibited catalytic activity after this treatment (Figure 19), LCMS analysis could not successfully identify an associated ligand. Thus, while a natural inhibitor of IspD may indeed be present in the library (possibly in low abundance), it is plausible that enzymatic denaturation of IspD may also account for the observed decline in activity. None-the-less, the quantitative binding of fosmidomycin to IspC illustrates the potential of bioprospecting as an alternative to HTS and encourages further study and screening with IspD.

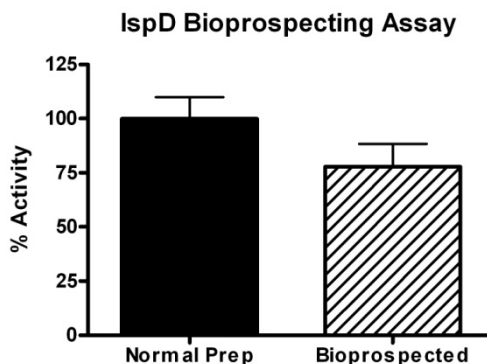


**Figure 19 - The IspD assay reported approximately 25% less specific activity after the enzyme was exposed to the test library.**

## Conclusion

The MEP pathway is an attractive target for novel drugs because of its prevalence in many pathogenic organisms but not in humans. This study characterized and validated IspD of *Francisella tularensis* as a strong target candidate for drug development. The first steps in drug discovery are target identification and validation, followed by lead compound identification and optimization, and lastly clinical trials. *F. tularensis* IspD was identified as a target based on the observation that MEP pathway knockouts are lethal [10], and this project characterized the enzyme by a number of criteria to validate it as an attractive target for antibiotics. Some of the most well studied homologs of IspD are from *E. coli* and *M. tuberculosis*, with which FtIspD has 34% and 25% homology to, respectively. Few other homologs have been characterized in the literature, and this was the first study of *F. tularensis* IspD to be published. FtIspD kinetic values are similar to the values reported for other homologs in the literature, and furthermore the assay could be scaled down to a high throughput screen format.

The regulation of metabolic flux through the MEP pathway is poorly understood. The MEP pathway appears to be regulated by several enzymes, with evidence indicating that the early and late steps of the pathway are most regulated [18]. Phosphorylation as a regulatory mechanism of the pathway has not been reported. Threonine 141 is an

accessible residue that is a key component of the cytidylation reaction in FtlIspD and the observation that it may be phosphorylated may suggest a mechanism by which the regulation of IspD contributes to overall rate limitation of the MEP pathway. Finally, lead compounds for IspD inhibitors may be discovered through bioprospecting and may reduce the costs associated with high throughput. This method was validated by capturing fosmidomycin with IspC, while further experiments may uncover a source of an inhibitor for IspD.

## References

## References

1. M. Friend (2006). Tularemia. *United States Geological Survey Circular 1297*, Reston, VA.
2. B. Cunha (2009). Tularemia. *The Merck Manual* (Online).  
<http://www.merckmanuals.com/professional/sec14/ch173/ch173r.html>
3. K. Feldman, R. Enscoe, S. Lathrop, B. Matyas, M. McGuill, M. Schrieffer, D. Stiles-Enos, D. Dennis, L. Petersen, E. Hayes (2001). An Outbreak of Primary Pneumonic Tularemia on Martha's Vineyard. *N. Engl. J. Med.* 345(22): 1601-1606.
4. K. Feldman, D. Stiles-Enos, K. Julian, B. Matyas, S. Telford III, M. Chu, L. Petersen, E. Hayes (2003). Tularemia on Martha's Vineyard: Seroprevalence and Occupational Risk. *Emerg. Infect. Dis.* 9(3): 350-354.
5. J. Hudspeth (2005). *Francisella tularensis*. In G. Zubay (Ed.) *Agents of Bioterrorism*, (p 44). New York: Columbia.
6. H. Eoh, P. Brennan, D. Crick (2009). The *Mycobacterium tuberculosis* MEP (2C-methyl-D-erythritol 4-phosphate) pathway as a new drug target. *Tuberculosis*. 89: 1-11.
7. J. Gershenzon, N. Dudareva (2007) The function of terpene natural products in the natural world. *Nat. Chem. Biol.* 3: 408-414.
8. B. Agranoff, H. Eggerer, U. Henning, F. Lynen (1959) Isopentenol Pyrophosphate Isomerase. *Journal of the American Chemical Society* 81: 1254-1255.
9. M. Rohmer, M. Knani, P. Simonin, B. Sutter, H. Sahm (1993). Isoprenoid biosynthesis in bacteria: a novel pathway for the early steps leading to isopentenyl diphosphate. *Biochem. J.* 295: 517-524.

10. L. Gallagher, E. Ramage, M. Jacobs, R. Kaul, M. Brittnacher, C. Manoil (2006) A comprehensive transposon library of *Francisella novicida*, a bioweapon surrogate. *PNAS* 104(3): 1009-1014.
11. R. Dhiman, M. Schaeffer, A. Bailey, C. Testa, H. Scherman, D. Crick. (2005) 1-Deoxy-D-Xylulose 5-Phosphate Reductoisomerase (IspC) from *Mycobacterium tuberculosis*: towards Understanding Mycobacterial Resistance to Fosmidomycin. *J. Bacteriol.* 187(24): 8395-8402.
12. A. Lillo, C. Tetzlaff, F. Sangari, D. Cane (2003). Functional Expression and Characterization of EryA, the Erythritol Kinase of *Brucella abortus*, and Enzymatic Synthesis of L-Erythritol-4-phosphate. *Bioorg. & Med. Chem. Lett.* 13: 737-739.
13. D.E. Cane, C. Chow, A. Lillo, I. Kang (2001). Molecular cloning, expression and characterization of the first three clones in the mevalonate-independent isoprenoid pathway in *Streptomyces coelicolor*. *Bioorg. Med. Chem.* 9: 1467-1477.
14. F. Rohdich, J. Wungsintaweekul, M. Fellermeier, S. Sagner, S. Herz, K. Kis, W. Eisenreich, A. Bacher, M. Zenk (1999) Cytidine 5'-triphosphate-dependent biosynthesis of isoprenoids: YgbP protein of *Escherichia coli* catalyzes the formation of 4-diphosphocytidyl-2-C-methylerythritol. *PNAS* 96(21): 11758-11763.
15. S. Richard, A. Lillo, C. Tetzlaff, M. Bowman, J. Noel, D. Cane (2004). Kinetic Analysis of *Escherichia coli* 2-C-Methyl-D-erythritol-4-phosphate Cytidyltransferase, Wild Type and Mutants, Reveals Roles of Active Site Amino Acids. *Biochemistry*, 43: 12918 -12917.
16. M. Cassera, F. Gozzo, F. D'Alexandri, E. Merino, H. del Portillo, V. Peres, I. Almeida, M. Eberlin, G. Wunderlich, J. Wiesner, H. Jomaa, E. Kimura, A. Katzin (2004). The Methylerythritol Phosphate Pathway is Functionally Active in All Intraerythrocytic Stages of *Plasmodium falciparum*. *J. Biol. Chem.* 279(50): 51749-51759.
17. C. Botté, F. Dubar, G. McFadden, E. Maréchal, C. Biot (2011) *Plasmodium falciparum* Apicoplast Drugs: Targets or Off-Targets? *Chemical Reviews*. Article ASAP: 10.1021/cr200258w.
18. M. Rodriguez-Concepcion (2006). Early steps in isoprenoid biosynthesis: Multilevel regulation of the supply of common precursors in plant cells. *Phytochem. Reviews* 5: 1-15.

19. M. Rohmer. (2008). From Molecular Fossils of Bacterial Hopanoids to the Formation of Isoprene Units: Discovery and Elucidation of the Methylerythritol Phosphate Pathway. *Lipids*. 43: 1095-1107.
20. H. Kojo, Y. Shigi, M. Nishida (1980). FR-31564, a New Phosphonic Acid Antibiotic: Bacterial Resistance and Membrane Permeability. *J. Antibiot.* (Tokyo). 33: 44-48.
21. B. Zhang, K. Watts, D. Hodge, L. Kemp, D. Hunstad, L. Hicks, A. Odom (2011). A Second Target of the Antimalarial and Antibacterial Agent Fosmidomycin Revealed by Cellular Metabolic Profiling. *Biochemistry*. 50: 3570-3577.
22. L. Deng, K. Endo, M. Kato, G. Cheng, S. Yajima, Y. Song (2011) Structures of 1-deoxy-D-xylulose-5-phosphate reductoisomerase/lipophilic phosphonate complexes. *ACS Med. Chem. Lett.* 2: 165-170.
23. Y. Sakamoto, S. Furukawa, H. Ogihara, M. Yamasaki (2003) Fosmidomycin resistance in adenylate cyclase deficient (*cya*) mutants of *Escherchia coli*. *Biosci. Biotechnol. Biochem.* 67(9): 2030-2033.
24. A. Brown, T. Parish (2008) Dxr is essential in *Mycobacterium tuberculosis* and fosmidomycin resistance is due to lack of uptake.
25. N. Dharia, A. Sidhu, M. Cassera, S. Westenberger, S. Bopp, R. Eastman, D. Plouffe, S. Batalov, D. Park, S. Volkman, D. Wirth, Y. Zhou, D. Fidock, E. Winzeler (2009). Use of high-density tiling microarrays to identify mutations globally and elucidate mechanisms of drug resistance in *Plasmodium falciparum*. *Genome Biol.*, 10(2): R21.
26. P. Proteau (2004) 1-Deoxy-D-xylulose 5-phosphate reductoisomerase: an overview. *Bioorg. Chem.* 32: 483-493.
27. S. Jawaid, H. Seidle, W. Zhou, H. Abdirahman, M. Abadeer, J. Hix, M. van Hoek, R.D. Couch (2009) Kinetic Characterization and Phosphoregulation of the *Francisella tularensis* 1-Deoxy-D-Xylulose 5-Phosphate Reductoisomerase (MEP Synthase). *PLoS One* 4(12): e8280.
28. M. Tang, S.I. Odejinmi, Y.M. Allette, H. Vankayalapati, K. Lai (2011) Identification of novel small molecule inhibitors of 4-diphosphocytidyl-2-C-methyl-D-erythritol (CDP-ME) kinase of Gram-negative bacteria. *Bioorg. Med. Chem.* 19: 5886-5895.
29. J. Geist, S. Lauw, V. Illarionova, B. Illarionov, M. Fischer, T. Gräwert, F. Rohdich, W. Eisenreich, J. Kaiser, M. Groll, C. Scheurer, S. Wittlin, J. Alonso-



- Gómez, W.B. Schweizer, A. Bacher, F. Diederich (2010) Thiazolopyrimidine inhibitors of 2-methylerythritol 2,4-cyclodiphosphate synthase (IspF) from *Mycobacterium tuberculosis* and *Plasmodium falciparum*. *Chem. Med. Chem.* 5(7): 1092-1101.
30. C. Bernal, C. Palacin, A. Boronat, S. Imperial (2004). A colorimetric assay for the determination of 4-diphosphocytidyl-2-C-methyl-D-erythritol-4-phosphate synthase activity. *Anal. Biochem.* 337: 55-61.
  31. H. Eoh, A. Brown, L. Buetow, W. Hunter, T. Parish, D. Kaur, P. Brennan, D. Crick (2007) Characterization of the *Mycobacterium tuberculosis* 4-diphosphocytidyl-2-C-methyl-D-erythritol synthase: Potential for drug development. *J. Bacteriol.* 189(24): 8922-8927.
  32. M. Gabrielsen, C. Bond, I. Hallyburton, S. Hecht, A. Bacher, W. Eisenreich, F. Rohdich, W. Hunter (2004) Hexameric assembly of the bifunctional methylerythritol 2,4-cyclodiphosphate synthase and protein-protein associations in the deoxy-xylulose-dependent pathway of isoprenoid precursor biosynthesis. *J. Biol. Chem.* 279(50): 52753-52761.
  33. J. Perez-Gil, M. Bergua, A. Boronat, S. Imperial (2010) Cloning and functional characterization of an enzyme from *Helicobacter pylori* that catalyzes two steps of the methylerythritol phosphate pathway for isoprenoid biosynthesis. *Biochim. Biophys. Acta* 1800(9): 919-928.
  34. RCSB Protein Data Bank. 1i52, 1ini, 1inj  
Richard, S., Bowman, M., Kwiatkowski, W., Kang, I., Chow, C., Lillo, A., Cane, D., Noel, J. (2001). Structure of 4-diphospho-2-C-methylerythritol synthase involved in mevalonate-independent isoprenoid biosynthesis. *Nature Struct. Biol.* 8: 641-648. <http://www.rcsb.org>
  35. A. Tsang, H. Seidle, S. Jawaid, W. Zhou, C. Smith, R.D. Couch (2011). *Francisella tularensis* 2-C-Methyl-D-Erythritol 4-Phosphate Cytidylyltransferase: Kinetic Characterization and Phosphoregulation. *PLoS One* 6(6): e20884.
  36. J. Zhang, T. Chung, K. Oldenburg (1999). A Simple Statistical Parameter for Use in Evaluation and Validation of High Throughput Screening Assays. *J Biomol Screen.* 4(2): 67-73.
  37. V. Samygina, A. Popov, E. Rodina, N. Vorobyeva, V. Lamzin, K. Polyakov, S. Kurilova, T. Nazarova, S. Aveava (2001). The Structures of Escherichia coli Inorganic Pyrophosphatase Complexed with Ca<sup>2+</sup> or CaPPi at Atomic Resolution and their Mechanistic Implications. *J. Mol. Biol.* 314: 633-645.

38. T. Johannes, M. DeSieno, B. Griffin, P. Thomas, N. Kelleher, W. Metcalf, H. Zhao (2010) Deciphering the late biosynthetic steps of antimalarial compound FR-900098. *Chem. Biol.* 17: 57-64.
39. S. Richard, M. Bowman, W. Kwiatkowski, I. Kang, C. Chow, A. Lillo, D. Cane, J. Noel (2001). Structure of 4-diphospho-2-C-methylerythritol synthase involved in mevalonate-independent isoprenoid biosynthesis. *Nature Struct. Biol.* 8: 641-648.
40. W. Shi, J. Feng, M. Zhang, X. Lai, S. Xu, X. Zhang, H. Wang (2007) Biosynthesis of isoprenoids: characterization of a functionally active recombinant 2-C-methyl-D-erythritol 4-phosphate cytidylyltransferase (IspD) from *Mycobacterium tuberculosis* H37Rv. *J. Biochem. Mol. Biol.* 40(6): 911-920.
41. A. Roy, A. Kucukural, Y. Zhang (2010) I-TASSER: a unified platform for automated protein structure and function prediction. *Nature Protocols*, 5: 725-738.
42. Y. Zhang (2008) I-TASSER server for protein 3D structure prediction. *BMC Bioinformatics*, 9(40).
43. B. Wallner, A. Elofsson (2005) Identification of correct regions in protein models using structural, alignment and consensus information. *Protein Sci.*, 15(94): 900-913.

## **Curriculum Vitae**

Arthur K. Tsang received his Bachelor of Science in Chemistry with a concentration in Biochemistry from George Mason University in 2009.